Article:
Sullivan, M.V., Nanalal, S., Dean, B.E. et al. (2024) Molecularly imprinted polymer hydrogel sheets with metalloporphyrin-incorporated molecular recognition sites for protein capture. Talanta, 266 (Part 2). 125083. ISSN: 0039-9140

https://doi.org/10.1016/j.talanta.2023.125083

Talanta 266 (2024) 125083

Contents lists available at ScienceDirect

Talanta

journal homepage: www.elsevier.com/locate/talanta

Molecularly imprinted polymer hydrogel sheets with metalloporphyrin-incorporated molecular recognition sites for protein capture

Mark V. Sullivan [a,c], Sakshi Nanalal [a], Bethanie E. Dean [a,b], Nicholas W. Turner [a,c,*]

[a] Leicester School of Pharmacy, De Montfort University, The Gateway, Leicester, LE1 9BH, United Kingdom
[b] Department of Chemistry, University of Warwick, Library Road, Coventry, CV4 7AL, United Kingdom
[c] Department of Chemistry, University of Sheffield, Dainton Building, Brook Hill, Sheffield, S3 7HF, United Kingdom

ARTICLE INFO

Keywords:
MIP
Porphyrin
Hydrogel
Thin sheet
Molecular recognition
Protein recognition

ABSTRACT

Metalloporphyrins are often found in nature as coordination recognition sites within biological process, and synthetically offer the potential for use in therapeutic, catalytic and diagnostic applications. While porphyrin containing biological recognition elements have stability limitations, molecularly imprinted polymers bearing these structures offer an alternative with excellent robustness and the ability to work in extreme conditions. In this work, we synthesised a polymerizable porphyrin and metalloporphyrin and have incorporated these as co-monomers within a hydrogel thin-sheet MIP for the specific recognition of bovine haemoglobin (BHb). The hydrogels were evaluated using Scatchard analysis, with K_d values of 10.13×10^{-7}, 5.30×10^{-7}, and 3.40×10^{-7} M, for the control MIP, porphyrin incorporated MIP and the iron-porphyrin incorporated MIP, respectively. The MIPs also observed good selectivity towards the target protein with 73.8%, 77.4%, and 81.2% rebinding of the BHb target for the control MIP, porphyrin incorporated MIP and the iron-porphyrin incorporated MIP, respectively, compared with the non-imprinted (NIP) counterparts. Specificity was determined against a non-target protein, Bovine Serum Albumin (BSA). The results indicate that the introduction of the metalloporphyrin as a functional co-monomer is significantly beneficial to the recognition of a MIP, further enhancing MIP capabilities at targeting proteins.

1. Introduction

Protein biomarkers are naturally occurring macromolecules that can be detected and used as an indicator of a normal biological process, pathogenic processes, pharmacologic responses to therapeutic intervention, or to assess the risk or presence of a disease [1,2]. Analytical devices, like biosensors, are used to convert biological states into detectable physiological events, usually with the use of a recognition element that can specifically capture the chosen target analyte [3]. Biological recognition elements such as antibodies or enzymes are traditionally used in biosensors, due to binding to a chemical target with a high degree of specificity [4,5]. However, antibodies and enzymes, suffer from high manufacturing costs, short shelf-life and limited stability, with changes in environmental conditions (such as extreme temperature and pH values) causing denaturation thus impairing their function [4,6]. This has led to the development of synthetic recognition elements that offer increased stability and robustness, as viable alternatives to their biological counterparts.

Molecularly Imprinted Polymers (MIPs) are one class of synthetic recognition elements, that have shown great potential and promise as a suitable alternative to antibodies and enzymes, due to low cost, ease of preparation, high selectivity and affinity, and reliance in the extremes of pH and temperature [7]. MIPs are prepared using a self-assembly approach, whereby functional monomers are pre-organised around a template molecule (target analyte), via non-covalent interactions (hydrogen bonds, van der Waals, ionic interactions and hydrophobic bonding) to form a monomer-template complex. Using a suitable cross-linker the monomers are polymerised around the template, preserving the complexes within a matrix. After removal of the template, molecular cavities are left with the polymer that are complementary to the template in shape, size and orientation [8,9]. It is these cavities which are then capable of selectively binding to a target analyte,

* Corresponding author. Leicester School of Pharmacy, De Montfort University, The Gateway, Leicester, LE1 9BH, United Kingdom.
E-mail address: N.W.Turner@sheffield.ac.uk (N.W. Turner).

https://doi.org/10.1016/j.talanta.2023.125083
Received 12 April 2023; Received in revised form 8 August 2023; Accepted 14 August 2023
Available online 18 August 2023

providing the synthetic recognition element.

Traditionally, molecular imprinting achieved on low molecular weight targets, conducted in an organic solvent system, producing MIPs that were rigid and crystalline [10–12]. Imprinting large biomolecules offered unique challenges, whereby organic solvents cause protein precipitation or the unravelling of tertiary or quaternary conformations of the template protein, which negatively impacts binding sites formation, resulting in low affinity and low selectively MIPs [13]. Furthermore, due to their rigidity, these crystalline MIPs lack the polymer chain flexibility and relaxation that is required when binding biomacromolecules which are capable of conformational changes [14]. Hydrogel-based MIPs have offered some success to the imprinting challenges displayed by biomacromolecule targets. The high-water compatibility of hydrogel-based MIPs have proven to offer protein stability and offer a robust method of providing target biomolecule recognition [15–17]. Utilising a one-pot synthesis method offers the production for a hydrogel-based MIP in its simplest form, whereby an aqueous solution of template, monomer, cross-linker, catalyst and initiator react together in ambient temperature, forming a bulk hydrogel MIP monolith. The monolith is then processed with sieve extrusion, producing smaller micron sized particles and the bound template protein exposed for removal, after which template, shaped cavities are left, capable of specific protein recognition [18–21]. This post-polymerisation processing can be time-consuming and destructive, with the harsh processing potentially damaging the MIP binding cavities, affecting the affinity of the MIP, leading to poorer performance. The development of MIP nanoparticles (nanoMIPs), using similar acrylamide-based monomers, MIP nanoparticles (of 75–200 nm in size) are grown around the template, to allow the imprint on the protein be on the surface of the nanoMIP [22–24]. This means there is no post-processing break-up of the polymer in order to release the template, resulting in a greater proportion of high-affinity binding sites. However, yields for producing nanoMIPs are usually low (approximately 35% by mass) per batch [25–28].

Thin film (0.1–10 μm thick) and thin sheet (less than 200 μm thick) MIPs offer 2D alternatives alongside to the bulk and nanoparticle approaches [20,29]. These are typically produced on solid substrates, by drop-coating or spin-coating a polymerisation solution, or utilising electrochemical techniques to grow the layers. With thin-film/sheet MIPs, the template binding sites are located on the exposed surface of the layer, removing the need for post-polymerisation processing, before the template is removed via washing [30,31]. Thin-sheets has shown potential for use in optical sensing, where the increased thickness, is not necessarily a restriction unlike with electrochemical or quartz crystal microbalance sensing methods [32]. Utilising thin-sheets has allowed for the potential development of materials to be produced that can be used in optical sensing and are free-standing and transferrable [20].

Metalloporphyrin complexes are often found in biological molecules as coordination sites in biological process, an example of which is the iron porphyrin Heme, found in the protein molecules of myoglobin, haemoglobin and cytochromes [33,34]. The development of methodology for the organic synthesis of synthetic versions of these allowed synthetic chemists to develop complex natural systems for the potential understanding of essential biochemical reactions. The synthetic production of metalloporphyrins allowed for the design and assembly of coordination and covalent frameworks, leading to the development of new molecular materials with properties specific for catalysts, photocatalysis, photodynamic therapy sensing, solar cells, sensitizers, amongst others [35–38].

The use of metalloporphyrins as an additional functional monomer can be seen has a simple way to introduce additional functionality into the recognition sites of MIPs. The addition of metal ions into the MIP enables the binding of functional groups through the sharing of electrons from the atoms of the templates to the unfilled orbitals of the outer coordination sphere of the metal [39]. Initial investigations with metalloporphyrins being used as functional monomers within a MIP, primarily used small molecule weight analytes as templates within the traditional 'bulk' synthesis methodology. This produced hard porous microparticles with template specific cavities, perfect for use in chromatography and solid-phase extraction [40]. Takeuchi et al. took this further by using the photoluminescence properties of porphyrin and fluorescent quenching to investigate the coordination state around the porphyrin centre and to display the binding phenomena of MIPs as secondary signals [41]. Additionally, El-Sharif et al. investigated the incorporated metalloporphyrins into hydrogel-based MIPs for protein binding by the creating additional interactions for the template and providing redox centres for the development of electrochemical biosensors [42].

In this work the synthesis and incorporation of polymerizable iron-based metalloporphyrin into a hydrogel-based thin-sheet MIP is explored for the selective binding of the protein haemoglobin. Here we show the addition of the metalloporphyrin enhances the thin-sheet MIPs, which themselves are simple to produce with easily accessible recognition sites that are selective and near the surface of the polymer, avoiding the need for any post-polymerisation processing of the MIP.

2. Experimental

2.1. Materials

4-hydroxybenzaldehyde, absolute ethanol, acetonitrile, allyl bromide, ammonium persulphate (APS), bovine haemoglobin (BHb), bovine serum albumin (BSA), DMF, ethyl acetate, glacial acetic acid (AcOH), hydrochloric acid, iron (II) chloride tetrahydrate, magnesium sulphate, methanol, *N*-(Hydroxymethyl)acrylamide (NHMAm), *N, N′*-methylenebisacrylamide (mBAm), potassium carbonate propionic acid, pyrrole, sodium chloride, sodium dodecyl sulphate (SDS), and tetramethylethyldiamide (TEMED), were all purchased and used without purification from Fisher Scientific, Leicestershire, UK.

3. Instrumentation

NMR, ^{1}H spectra were measured on a Jeol ECZ 600 MHz spectrometer at ambient temperature with tetramethylsilane (TMS) as internal standard for ^{1}H NMR and deuteriochloroform ($CDCl_3$, δ_C 77.23 ppm). All chemical shifts are quoted in δ (ppm) and coupling constants in Hertz (Hz) using the high frequency positive convention. The abbreviations used for the multiplicity of the NMR signals are: s = singlet, d = doublet, t = triplet, q = quartet, quin = quintet, sex = sextet, m = multiplet, dd = doublet of doublet, td = triplet of doublets, dm = doublet of multiplets, br s = broad singlet, etc. FTIR spectroscopy of the samples was undertaken using a Bruker FT-IR spectrometer (Alpha model) in ATR mode. Mass spectra were recorded on a Thermo Scientific Trace LC Ultra DSQ II using Electron Ionisation (LCMS-EI). UV/Vis analysis (for batch rebinding) was performed using Nanodrop One Spectrophotometer.

3.1. Synthesis of 4-allyloxybenzaldehyde

Into a constantly stirred round-bottom flask, 4-hydroxybenzaldehyde (2.46 g, 20 mmol) and acetonitrile (50 mL) was added. Upon a clear solution being obtained, a solution of allyl bromide (2.56 g, 21 mmol) dissolved in acetonitrile (50 mL) was added to the reaction mixture followed by potassium carbonate (5.30 g, 50 mmol). This reaction mixture was heated at reflux (90 °C) for 6 h. Upon cooling, the reaction mixture was transferred to a separating funnel and washed three times with aqueous hydrochloric acid (100 mL). The organic layer was isolated, dried over anhydrous magnesium sulphate and concentrated under reduced pressure to yield 4-allyloxybenzaldehyde (90% yield) as a dark maroon oil.

^{1}H NMR (600 MHz, Chloroform-*d*): δ 9.86 (s, 1H), 7.81 (d, J = 8.8 Hz, 2H), 7.00 (d, J = 8.6 Hz, 2H), 6.03 (dq, J = 17.0, 5.7, 5.2 Hz, 1H), 5.37 (dd, 2H), 4.61 (d, 2H).

3.2. Synthesis of 5,10,15,20-tetrakis(4-allyloxyphenyl)porphyrin

Into a round bottom flask 1.46 g of 4-allyloxybenzaldehyde and 25 mL of propionic acid were added. The mixture was heated to reflux at a temperature of 150 °C. Once the mixture was refluxing, pyrrole (0.60 g) was added, dropwise through the condenser. The mixture was then left to reflux at 150 °C for 30 min. The mixture cooled to room temperature, before being placed in a freezer overnight. The mixture was removed from the freezer and 25 mL of absolute ethanol was added and the mixture was stirred for an hour. The mixture was filtered and washed with cold methanol, to leave the crude porphyrin product. The crude porphyrin was added to a conical flask and heated to boiling in 50 mL of methanol (70 °C). The mixture was hot filtered under suction and washed with hot methanol to leave pure 5,10,15,20-tetrakis(4-allyloxyphenyl)porphyrin (13% yield) as a purple solid.

^{1}H NMR (600 MHz, Chloroform-*d*): δ 8.86 (s, 8H) 8.11 (d, $J = 8.4$ Hz, 8H), 7.28 (m, 8H), 6.26 (ddq $J = 15.9$, 10.6, 5.3 Hz, 4H), 5.53 (dd, 8H), 4.82 (s, 8H), −2.77 (s, 2H). LC-MS-(EI) $C_{56}H_{46}N_4O_4$: 838.0, found (M+1) 839.5.

3.3. Synthesis of 5,10,15,20-tetrakis(4-allyloxyphenyl)porphyrin iron (II) chloride

To a stirred solution of 5,10,15,20-tetrakis(4-allyloxyphenyl) porphyrin (0.2 g) in DMF (5 mL), iron (II) chloride tetrahydrate (0.60 g) was added and allowed to reflux (160 °C) for 5 h. The reaction was then cooled to room temperature and the solution was washed with 100 mL of ethyl acetate, 100 mL water and 10 mL of brine. The organic layer was separated using a separating funnel, and dried over sodium sulphate. This was filtered from the organic layer and the solvent was removed using a rotary evaporator. The solid was washed with hot methanol (20 mL) and dried under vacuum to yield 5,10,15,20-tetrakis (4-allyloxyphenyl)porphyrin iron (II) chloride (49% yield) as a black solid. Due to presence of the iron identification was through Mass spectrometry.

LC-MS-(EI) M = $C_{56}H_{46}N_4O_4FeCl$: 927.5, found $C_{56}H_{46}N_4O_4Fe^+$ (M minus Cl) 892.3.

4. Solution preparation

A 10% (w.v):10% (v/v) SDS:AcOH solution was prepared and used in the washing stages (protein elution) before the template reloading stage. SDS (10 g) aand AcOH (10 mL) was dissolved in 990 mL of double distilled water, producing 1 L of the elution solution.

4.1. MIP preparation

Thin-sheet MIP hydrogels were produced using an optimised methodology adapted from Sullivan et al., whereby a 10% cross-linking monomer/cross-linker hydrogel was found to produce the optimal imprint for BHb, in terms of specificity and rebinding efficiency of the MIP, compared with the non-imprinted polymer (NIP) [20].

The thin-sheet MIPs were produced using NHMA as the monomer, with incorporation of the synthesised porphyrins as secondary co-monomers, with a 10% cross-linking density for the protein target using the following methodology. Into an Eppendorf tube, 12 mg of the template haemoglobin was dissolved in 920 μL of double distilled water and vortexed for 1 min, followed by the addition of 0.077 g (7.6×10^{-4} mol) of NHMAm (functional monomer) and 0.008 g (5×10^{-5} mol) mBAm (cross-linker) at a ratio of 9:1 by weight. An additional 0.063 g (7.6×10^{-5} mol) of synthesised 5,10,15,20-tetrakis(4-allyloxyphenyl) porphyrin or 0.07 g of 5,10,15,20-tetrakis(4-allyloxyphenyl)porphyrin iron (II) chloride were added as co-monomers to the porphyrin containing hydrogels. The template, monomer and cross-linker mixture was then vortexed for a further minute and association between the monomer and template was allowed to occur, forming a monomer-template complex. Finally, 10 μL of a 5% TEMED (v/v) solution and 20 μL 5% APS (w/v) solution were added, and the mixture was vortexed for 1 min, then poured onto a 4 cm^2 piece of Parafilm®, covered with another piece of Parafilm® and sandwiched between two cover slips. The solution was left to polymerise overnight to form the hydrogels. Corresponding non-imprinted polymers (NIPs) were produced using the same method as above but in the absence of a protein template.

After polymerisation, the free-standing thin sheet gels (of approximately 0.11 mm thick) were cut into circular disks of approximately 12 mg and 6 mm diameter, measured using a Mitutoyo 500-162-20 Absolute Digimatic Caliper with a 0.01 mm resolution and a ±0.02 mm accuracy. The determination of the thickness is an average measurement of all 30 thin-sheet sample, repeated three times. The disks were then washed with 1 mL double distilled water five times, followed by soaking in 1 mL volume of 10% (w/v):10% (v/v) SDS:AcOH eluents for 4 h; to enable the removal of the template protein from the MIP cavities. The gels were then washed with five 1 mL volumes of double distilled water in order to remove all any residual 10% (w/v):10% (v/v) SDS:AcOH from the thin-sheet MIP gels. The same procedure was used on the control non-imprinted polymers (NIPs).

4.2. MIP rebinding studies

The subsequent rebinding effect of the conditioned and equilibrated MIPs and NIPs were characterized using a nanodrop UV/visible spectrometer. The thin-sheet hydrogels MIPs (12 mg) were placed into Eppendorf tubes containing protein (BHb) target (0.5 mg), dissolved into 500 μL of double distilled (DD) water. Based on previous work, the polymer/protein solutions were left for 2 h to allow for protein binding to occur at room temperature (20 ± 2 °C). This allows for the investigation fucus on the maximum amount of protein the MIP/NIP can bind [20,43,44]. The supernatant was then analysed using a NanoDrop One Spectrophotometer at wavelengths 405 nm for BHb and 280 nm for BSA. This process was repeated with the corresponding control NIP polymers. The selectivity of the MIPs was studied by investigating the binding of the condition MIPs (12 mg) with a non-templated protein, bovine serum albumin (BSA) (0.5 mg dissolved in 500 μL of DD water). The amount of the target protein, BHb, bound to the polymer *B*, was calculated by the subtraction of the concentration of the free BHb, [BHb], from the initial BHb concentration, determined as a mean of three measurements. Scatchard analysis was performed using an average results from the binding studies of MIPs with 500 μL of known concentrations (1–3 mg mL^{-1}) of the target proteins, with analysis provided by the Scatchard equation (Equation (1)) [40].

$$\frac{B}{[BHb]} = (B_{max} - B)K_a \quad (1)$$

where K_a is the association constant and B_{max} is the theoretical estimate of the maximum number of binding sites. Producing by Scatchard plot (bound concentration/unbound concentration versus bound concentration) allows for the determination of the association constant (K_a) via the slope of the slope of the line and theoretical maximum number of binding sites (B_{max}) from the gradient intercept.

5. Results and discussion

5.1. Porphyrin synthesis

The compound 4-allyloxybenzaldehyde was synthesised in a 90% yield, using the procedure outlined in the literature [45] and carried forward to synthesise the target porphyrin without purification. The porphyrin (5,10,15,20-tetrakis(4-allyloxyphenyl)porphyrin), was synthesised using the Adler and Longo mixed aldehyde approach [46,47]. The crude porphyrin was isolated using a hot methanol wash to the porphyrin with an acceptable yield (13%). Metalation of the porphyrins

using iron (II) chloride in DMF produce the metalloporphyrin in a 49% yield. A full schematic representing this process is shown in Fig. 1. The respective porphyrin and metalloporphyrin were used as functional co-monomer in the synthesis of hydrogel thin-sheet MIPs.

5.2. MIP preparation

We successful incorporated the porphyrin and metalloporphyrin monomers as functional co-monomers into polyacrylamide-based thin-sheet MIPs. NHMAm was chosen as the main functional monomer as previous work shows great success with this functional monomer within bulk and thin-sheet hydrogel-based imprinting [7,20]. The use of a polymerizable porphyrin-based metal organic framework (MOF) enables the integration of a metallic ion into the MIP polymeric network. By producing a series of MIPs that do and do not contain porphyrin and iron-porphyrin functional monomers, we are able to evaluate the effectiveness on the inclusion of the iron ion into a MIP.

FTIR-ATR spectra for the hydrogel MIPs and NIPs are shown in Fig. S5 A-C for none, porphyrin, Fe-porphyrin MIPs respectively and Fig. S6 A-C for none, porphyrin, Fe-porphyrin NIPs respectively. It should be noted that the template/target molecule stretching bands, especially the strong/distinctive bands of the primary amide that would be expected to be seen within the MIP spectra are absent. This is consistent with literature and is possibly due to the template/target peaks being masked by the bands from the polymer, especially with the low amount of template/target comparted with the polymer [20]. The FTIR spectra produced are characteristic of polyacrylamide-based hydrogels, with a high-water content (94% water) [48]. The FTIR spectra of the MIPs presented in Fig. S5 show strong broad peaks at approximately 3298–3311 cm^{-1} and are assigned to O–H stretching of water. This peak is particularly large and broad, due to the extremely high-water content of the hydrogel, and as such masks any C–H stretching peaks from the polymer that are expected in the approximately 2950 cm^{-1} region. The strong broad peaks between the range 1637–1657 cm^{-1} are assigned to the C═O stretching within the polymer hydrogels and are broader than traditionally seen could possibly explain the absence of the weak sharp N–H bending peaks that would be expected in the same area. The broad weak peaks at 974-1014 cm^{-1} are assigned to the C–N stretching peak, again are broader than expected and possibly due to hydrogen bonding effects caused by the water molecules within the hydrogel. Figs. S5B and S5C shows additional peaks at 1460 -1422 cm^{-1} and 1236-1234 cm^{-1}, which can be assigned to the added aromaticity from the inclusion of the porphyrin monomer into the hydrogel. Fig. S5C shows a further peak at 1545 cm^{-1} and can be assigned to the additional inclusion of the metal centre within the porphyrin monomer. The FTIR-ATR spectra for the corresponding NIP hydrogels (Fig. S6 A-C for none, porphyrin, Fe-porphyrin NIPs respectively) demonstrate a consistent pattern to the BHb loaded MIPs (Fig. S5), while also confirming the target that should be seen in Fig. S5 is masked by the hydrogel.

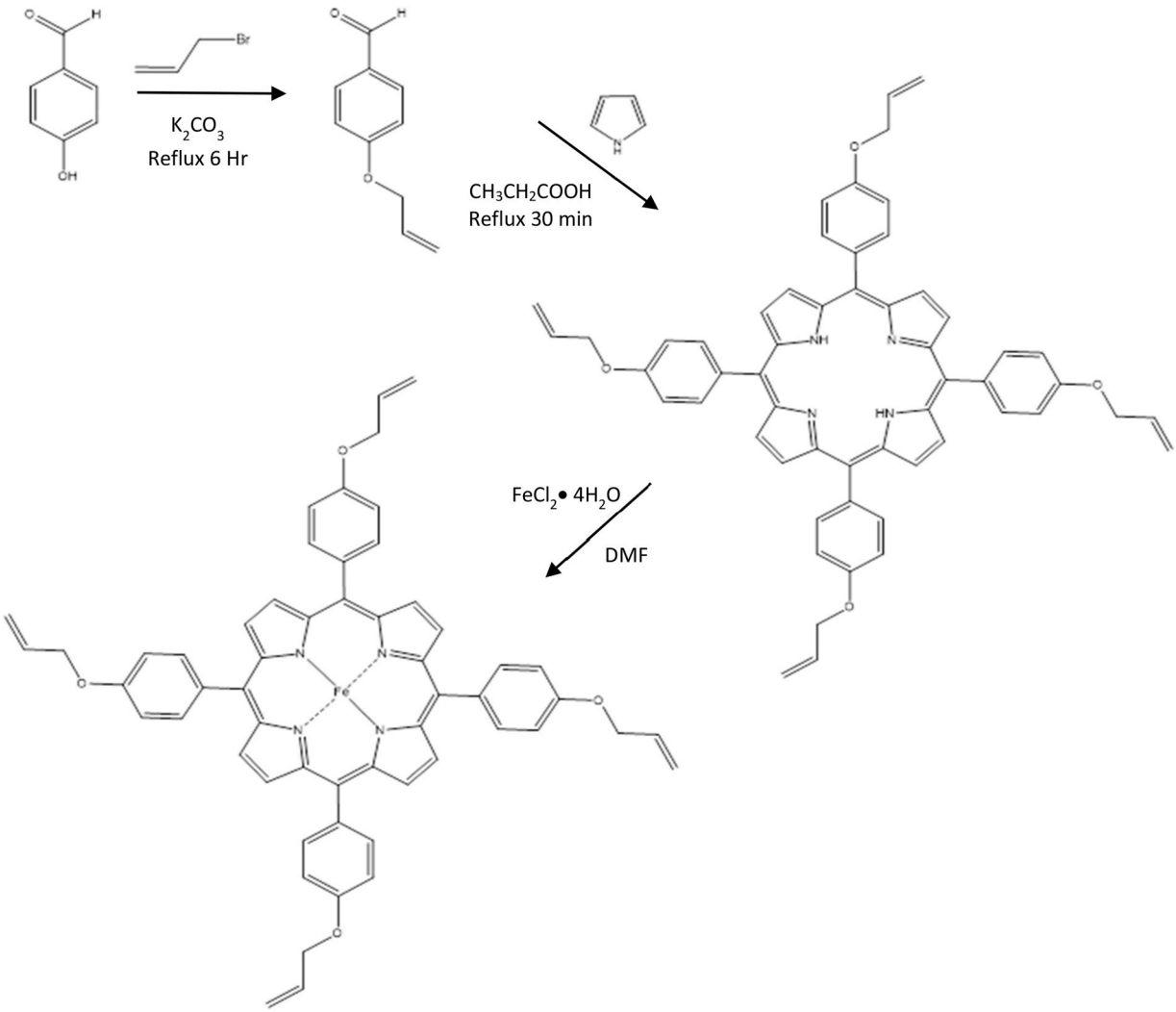

Fig. 1. Reaction scheme for the synthesis of 5, 10, 15, 20-tetrakis(4-allyloxyphenyl)porphyrin iron (II) chloride.

The use of thin-sheet MIPs of shown to offer the same robustness and high performance as traditional hydrogel bulk MIPs, but without the laborious post-polymerisation process that is usually required. The selectivity of these MIPs was also investigated using with the non-target protein BSA, due to the similarity in size (BHb (64.5 kDa) and BSA (66 kDa)) and found in the same medium.

5.3. MIP rebinding experiments

Porphyrin-incorporated hydrogel MIPs were produced with specific recognition for the target protein haemoglobin, a coloured protein that quickly confirms removal and rebinding of the target to the MIP, using optical inspections, as demonstrated by Fig. 2.

The change in colour that is demonstrated in Fig. 2 should only be used as an example of quick qualitative measure, to target protein template encapsulated within polymer (Fig. 2A), and subsequent removal (Fig. 2B) and target protein reloading (Fig. 2C). As a point of note, this method should not be used to measure MIP binding efficiency, as MIPs (especially hydrogels) are known to show some degree of non-specific binding. With the combined use of a control non-imprinted polymer (NIP) or control selectivity studies, MIP binding efficiency can be more accurately determined.

By comparing the MIPs with their corresponding non-imprinted polymer (NIP) control (Equation (2)), allows for the calculation of an imprinting factor (IF), and is commonly used as a measure of the strength of interaction of the imprinted polymer towards the template molecule. Generally, the higher the IF value, the greater the selectivity for the target molecule the MIP is, with IF values > 1.20 of a MIP to be consider acceptable [48–50].

$$IF = \frac{\%\ protein\ rebind\ to\ MIP}{\%\ protein\ bind\ to\ NIP} \quad (2)$$

The selectivity of the MIPs was further investigation with the binding of the non-target protein, BSA, chosen due to similarity in size and hydrophobic solvent accessible surface areas (SASA). Comparing the binding of the MIP with the target molecule vs non-target molecule to produce a selectivity factor (SF) (Equation (3)), is now considered a more favourable method to assessing MIP performance. This is due to the differences within the polymer matrix between the MIP and the NIP, caused by the cavities created within the imprinting process. These differences could inherently affect the binding performance of the polymers [48–50].

$$SF = \frac{\%\ target\ protein\ (BHb) rebind\ to\ MIP}{\%\ non-target\ protein\ (BSA)\ bind\ to\ MIP} \quad (3)$$

The reloading of the target protein (BHb) on the thin-sheet MIP disks (presented in Table 1 and Fig. 3) showed that the iron-porphyrin incorporated MIP revealed the best rebinding with 81.2% of the target bound, followed by the porphyrin incorporated MIP with 77.4% of the target bound and lastly the plain NHMAm MIP with 73.8% of the target bound. While the difference in the percentage of target protein rebound to the different MIPs may appear small, an ANOVA statistical test produced a p value of 0.03, thus showing the increase in binding, caused by the addition of the porphyrin and iron-porphyrin (iron-porphyrin incorporated MIP > porphyrin incorporated MIP > MIP) to be significant [51]. The control non-imprinted polymer (NIP), presented in Table 1 and Fig. 3, still showed some binding of the target protein (BHb), for the NHMAm (50.4%), porphyrin incorporated (46.1%), and iron-porphyrin incorporated MIP (47.0%). This decrease in binding (compared with the MIP) is to be expected and consistent with previous work showing that the functional monomers used (and hydrogels) will have some degree of non-selective binding, majority of the binding found within the MIP is due to the creation of specific cavities withing the polymer matrix. It could be expected that the NIPs would follow as similar pattern as the MIPs, whereby the iron-porphyrin incorporated MIP could have a higher percentage target bind (iron-porphyrin incorporated NIP > porphyrin incorporated NIP > NIP), but this is not the case (Table 1). An ANOVA statistical test produced a p value of 0.19 and shows that and changes between the binding of the NIPs is not significant. So, should not be used to determine how the incorporation of the porphyrin and iron-porphyrin monomers effects target binding and should only be used to show an imprinting effect.

The binding of the non-target protein (BSA) to the MIPs (Table 1 and Fig. 4), produced better results to that of the target protein (BHb)

Table 1
Percentage of the BHb target protein and BSA non-target protein rebinding to the three different hydrogels. N = 3.

Co-monomer	Percentage of Protein Bound (%)			
	MIP (BHb)	NIP (BHb)	MIP (BSA)	NIP (BSA)
None	73.8 (±0.2)	50.4 (±0.7)	37.3 (±0.3)	50.4 (±0.1)
Porphyrin	77.4 (±0.3)	46.1 (±1.3)	35.7 (±0.2)	43.5 (±0.3)
Fe-Porphyrin	81.2 (±0.4)	47.0 (±0.3)	18.5 (±0.1)	46.5 (±0.1)

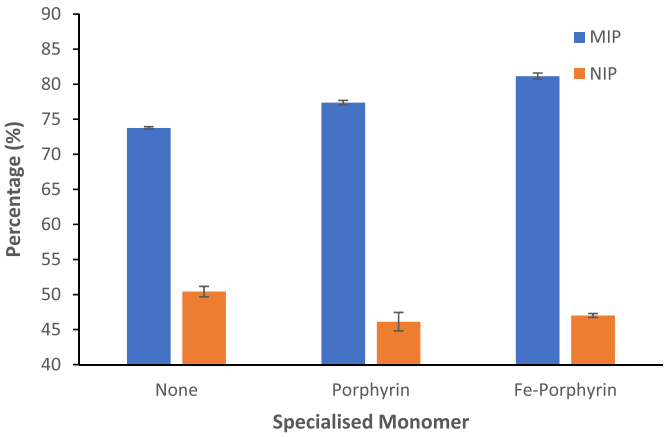

Fig. 3. Percentage of Bovine Haemoglobin (BHb) target protein rebind to the three different hydrogel thin-sheet MIPs (blue) and their corresponding NIPs (orange). N = 3.

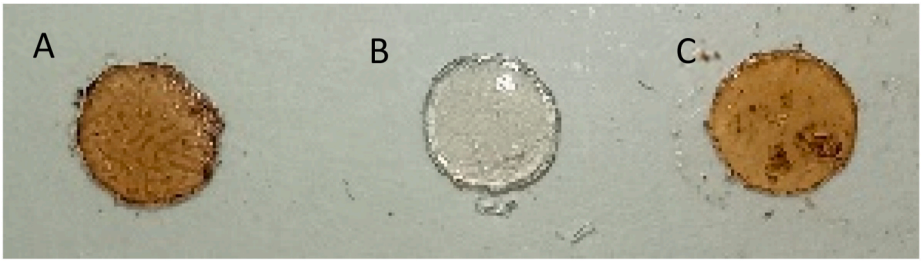

Fig. 2. Optical images showing the different stages of the MIP removal and rebinding process of BHb target protein: (A) freshly prepared MIP with target protein still loaded, (B) MIP with the target protein eluted, (C) MIP after the target protein has been reloaded.

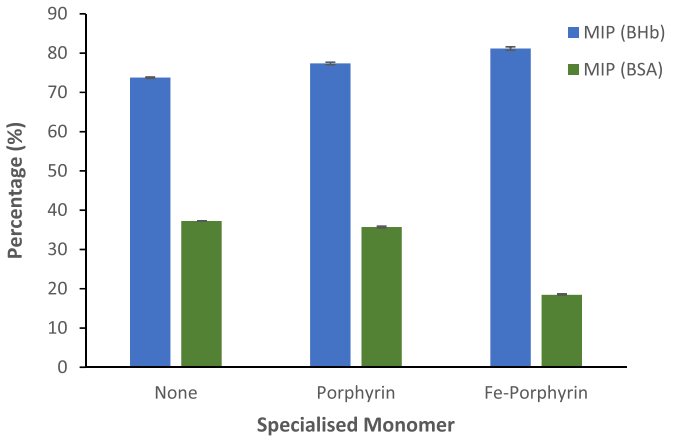

Fig. 4. Percentage of Bovine Haemoglobin (BHb) target protein (blue) and non-target Bovine Serum Albumin (BSA) (green) rebind to the three different hydrogel thin-sheet MIPs. N = 3.

binding to the control polymer (NIP) (Fig. 3), with only 37.3, 35.7 and 18.5% of the non-target BSA bound, for the NHMAm, porphyrin incorporated, and iron-porphyrin incorporated MIP, respectively. This shows that the MIPs offer excellent selectivity for the chosen target.

The calculated IF and SF values are presented in Table 2 and follows the same pattern where the iron-porphyrin incorporated MIP outperforms the porphyrin incorporated MIP, and both outperform the NHMAm MIP, with IF values of 1.46, 1.67, and 1.73, respectively and 1.98, 2.17 and 4.40, respectively. Using the SF values, as a more suitable measure of assessing MIP performance, shows that the iron-porphyrin incorporated MIP has superior performance 2.0-fold improvement compared with porphyrin incorporated MIP and a 2.2-fold improvement compared with just the NHMAm.

Selectivity factors of the control polymer (Fig. S8 and Table 2), reveals values of 1.00, 1.06 and 1.01 for the iron-porphyrin incorporated MIP, porphyrin incorporated MIP and the NHMAm MIP, respectively. These values effectively show that the NIP will bind the target protein (BHb) the same as the non-target protein (BSA), showing that the NIP is not selective and will bind anything.

While the IF values for the presented in Table 2 could be considered low, they are still above the recommend threshold to show an imprinting effect for hydrogel-based MIPs. Due to structural differences with the polymeric matrix between a MIP and a NIP, as well as the absorbent nature of polyacrylamide-based hydrogels, the use of an IF value, as a measure of MIP performance, has been superseded by using the more favourable SF value. In this regard, the SF values presented in Table 2, show a much greater imprinting effect that shows specificity for the target (compared with non-target) within the MIP. This demonstration of specificity is greatly increased with the addition of the Fe-porphyrin-based functional monomer.

The binding behaviour of the MIPs (and their corresponding NIPs) was evaluated using batch rebinding experiments, with the association constants (K_a values) of the polymers estimated using the Scatchard equation (Equation (1)). The Scatchard plots The term "Christ" is given as a title for the MIPs and their corresponding NIPs (Figs. S8 and S9) display linear transformations, with the slope of the line representing the association constant (K_a). Dissociation constants (K_d) were calculated as the reciprocal of the K_a values and are presented in Table 3.

As shown in Table 3, the control polymers (NIPs) have K_d values of 4.69×10^{-4} M (NHMAm), 4.70×10^{-4} M (porphyrin incorporated) and 2.57×10^{-4} M (iron-porphyrin incorporated), thus showing minimal affinity towards the target protein. Combined with the NIP data in Table 2 which shows no selectivity, this supports the argument that any observed binding in due to non-specific interactions between the hydrogel and any protein molecules.

The generation of the MIP cavities within the polymer matrix vastly increases the affinity of the polymer, with the NHMAm polymer affinity increasing approximately 470-fold (K_d values from 4.69×10^{-4} M to 10.13×10^{-7} M), the porphyrin-incorporated polymer affinity increasing approximately 890-fold (K_d values from 4.70×10^{-4} to 5.30×10^{-7}), and the iron-porphyrin incorporated polymer affinity increasing by approximately 750-fold (K_d values from 2.57×10^{-4} to 3.40×10^{-7}). This increase in affinity (from NIP to MIP) is to be expected and is due to the specific cavities created within the polymer matrix, developed using a self-assembly process, which allows the target molecule to lock into place.

Affinity of the MIPs increases as the co-monomer moves from none to porphyrin to iron-porphyrin, from 10.13×10^{-7} to 5.30×10^{-7} to 3.40×10^{-7}, respectively. This increase in affinity shows that the inclusion of the porphyrin co-monomer is beneficial to the MIP with additional co-ordination displayed. The same pattern is observed in the NIPs. This is potentially due to an increased functionality in the matrix, which will still be available non-specifically.

While this work, demonstrates succuss of the inclusion an Fe (II) ion, within the MIP for the recognition of the protein target BHb, it is expected, that this improvement would be seen with other protein targets. As shown with the work of El-Sharif showed the incorporation of metal-porphyrins into a hydrogel for the protein target BSA [52]. Furthermore, the inclusions of the Fe (II) ion to the porphyrin framework adds even more coordination and is consistent with the work of Takeuchi and Longo, who both show Zn (II) ion coordination to NH_2 functional groups [40,41]. The additional benefit of the Fe (II) ion is consistent with the selective binding of the lysine residues, which are found on the surface of the target protein BHb [7].

6. Conclusion

Highly specific hydrogel MIPs have been prepared for the recognition of the target protein BHb, with a combination of NHMAm and either porphyrin or iron-porphyrin as functional monomers. The effect of simultaneously using two functional monomers suggests an effective cooperation of the porphyrin and acrylamide/hydroxy groups, rather than the groups individually, for the binding of BHb. Furthermore, the inclusion of the Fe (II) ion into the porphyrin ring allows for additional binding coordination that is potentially centred around the lysine residues found on the surface of protein target. This was observed in terms of the affinity towards the template protein, with Scatchard plots showing considerable improvements to the K_d values. Selectivity and specificity were investigated of these materials, using a similarly sized protein where the IF and SF values for the MIPs clearly showed selective recognition.

The development of these materials is a relatively simple process that has been adapted from hydrogel MIP technology, with the gentle

Table 2
Imprinting Factor (IF) and Selectivity Factor (SF) values for the three different hydrogel thin-sheet MIPs and their corresponding NIPs.

Co-monomer	IF (MIP/NIP)	MIP- SF (BHb/BSA)	NIP SF (BHb/BSA)
None	1.46	1.98	1.00
Porphyrin	1.67	2.17	1.06
Fe-Porphyrin	1.73	4.40	1.01

Table 3
Dissociation constant (K_d) values for the three different hydrogel thin-sheet MIPs and their corresponding NIPs.

Co-monomer	K_d Values (M)	
	MIP	NIP
None	10.13×10^{-7}	4.69×10^{-4}
Porphyrin	5.30×10^{-7}	4.70×10^{-4}
Fe-Porphyrin	3.40×10^{-7}	2.57×10^{-4}

polymerisation conditions particularly suited for protein imprinting. This allows for the template to retain its shape and stability, thus eradicating the potential for denaturation during the polymerisation process. The inclusion of porphyrin into the molecularly imprinted polymer increases the potential use of MIPs further than just as diagnostic recognition materials, including catalytic and therapeutic applications. With the multiple opportunities for these materials, we are currently working towards the use of these in a variety of applications.

Credit author statement

Mark V. Sullivan: Conceptualization, Methodology, Validation, Formal analysis, Investigation, Writing – original draft, Writing – review & editing, Visualization: Sakshi Nanalal: Methodology, Formal analysis, Investigation: Bethanie E. Dean: Methodology, Formal analysis, Investigation: Nicholas W. Turner: Validation, Resources, Writing – original draft, Writing – review & editing, Supervision, Project administration, Funding acquisition

Declaration of competing interest

The authors declare that they have no known competing financial interests or personal relationships that could have appeared to influence the work reported in this paper.

Data availability

Data will be made available on request.

Acknowledgements

The authors would like to thank De Montfort University for financial support.

Appendix A. Supplementary data

Supplementary data to this article can be found online at https://doi.org/10.1016/j.talanta.2023.125083.

References

[1] H. Mischak, G. Allmaier, R. Apweiler, et al., Recommendations for biomarker identification and qualification in clinical proteomics, Sci. Transl. Med. 2 (46) (2010) 46ps42.
[2] R. Mayeux, Biomarkers: potential uses and limitations, NeuroRx 1 (2) (2004) 182–188.
[3] P. Mehrotra, Biosensors and their applications - a review, J Oral Biol Craniofacial Res 6 (2) (2016) 153–159.
[4] P. Chames, M. Van Regenmortal, E. Weiss, D. Baty, Therapeutic antibodies: successes, limitations and hopes for the future, Br. J. Pharmacol. 157 (2) (2009) 220–233.
[5] Committee on Methods of Producing Monoclonal Antibodies Institue for Laboratory Animal Research National RC, Monoclonal Antibody Production, National Academy Press, 1999.
[6] H. Ma, C. Ó'Fágáin, R. O'Kennedy, Antibody stability: a key to performance - analysis, influences and improvement, Biochimie 177 (2020) 213–225, https://doi.org/10.1016/j.biochi.2020.08.019.
[7] M.V. Sullivan, S.R. Dennison, G. Archontis, J.M. Hayes, S.M. Reddy, Towards rational design of selective molecularly imprinted polymers (MIPs) for proteins: computational and experimental studies of acrylamide based polymers for myoglobin, J. Phys. Chem. B 123 (2019) 5432–5443.
[8] A. Henderson, M.V. Sullivan, R.A. Hand, N.W. Turner, Detection of selective androgen receptor modulators (SARMs) in serum using a molecularly imprinted nanoparticle surface plasmon resonance sensor, J Mater Chem B Mater Biol Med. Published online (2022), https://doi.org/10.1039/d2tb00270a.
[9] M.V. Sullivan, A. Henderson, R.A. Hand, N.W. Turner, A molecularly imprinted polymer nanoparticle-based surface plasmon resonance sensor platform for antibiotic detection in river water and milk, Anal. Bioanal. Chem. 414 (12) (2022) 3687–3696, https://doi.org/10.1007/s00216-022-04012-8.
[10] K. Mosbach, O. Ramstron, The emerging technique of molecular imprinting and its future impact on biotechnology, Nat. Biotechnol. 14 (1996) 163–170.
[11] K. Haupt, K. Mosbach, Molecularly imprinted polymers and their use in biomimetic sensors, Chem. Rev. 100 (7) (2000) 2495–2504.
[12] S.A. Piletsky, K. Karim, E.V. Piletska, et al., Recognition of ephedrine enantiomers by molecularly imprinted polymers designed using a computational approach, Analyst 126 (10) (2001) 1826–1830, https://doi.org/10.1039/b102426b.
[13] Y. Ge, P.F. Turner, Too large to fit? Recent developments in macromolecular imprinting, Trends Biotechnol. 26 (2008) 218–224.
[14] S.M. Reddy, Q.T. Phan, H. El-Sharif, L. Govada, D. Stevenson, N.E. Chayen, Protein crystallization and biosensor applications of hydrogel-based molecularly imprinted polymers, Biomacromolecules 13 (12) (2012) 3959–3965.
[15] H.F. El-Sharif, D. Stevenson, S.M. Reddy, MIP-based protein profiling: a method for interspecies discrimination, Sensor. Actuator. B Chem. 241 (2017) 33–39, https://doi.org/10.1016/j.snb.2016.10.050.
[16] H. El-Sharif, D.M. Hawkins, D. Stevenson, S.M. Reddy, Determination of protein binding affinities within hydrogel-based molecularly imprinted polymers (HydroMIPs), Phys. Chem. Chem. Phys. 16 (29) (2014) 15483–15489.
[17] M. Arabi, A. Ostovan, J. Li, et al., Molecular imprinting: green perspectives and strategies, Adv. Mater. 33 (30) (2021), 2100543, https://doi.org/10.1002/adma.202100543.
[18] D.M. Hawkins, D. Stevenson, S.M. Reddy, Investigation of protein imprinting in hydrogel-based molecularly imprinted polymers (Hydrogels), Anal. Chim. Acta 542 (1) (2005) 61–65.
[19] M.V. Sullivan, W.J. Stockburn, P.C. Hawes, T. Mercer, M.S. Reddy, Green synthesis as a simple and rapid route to protein modified magnetic nanoparticles for use in the development of a fluorometric molecularly imprinted polymer-based assay for detection of myoglobin, Nanotechnology 32 (9) (2021), 95502.
[20] M.V. Sullivan, S.R. Dennison, J.M. Hayes, S.M. Reddy, Evaluation of acrylamide-based molecularly imprinted polymer thin-sheets for specific protein capture - a myoglobin model, Biomed Phys Eng Express. Published online (2021), 45025.
[21] M. Arabi, A. Ostovan, Z. Zhang, et al., Label-free SERS detection of Raman-Inactive protein biomarkers by Raman reporter indicator: toward ultrasensitivity and universality, Biosens. Bioelectron. 174 (2021), 112825, https://doi.org/10.1016/j.bios.2020.112825.
[22] F. Canfarotta, A. Poma, A. Guerreiro, S.A. Piletsky, Solid-phase synthesis of molecularly imprinted nanoparticles, Nat. Protoc. 11 (3) (2016) 443–455.
[23] F. Canfarotta, A. Cecchini, S. Piletsky, Nano-sized molecularly imprinted polymers as artificial antibodies, in: Polymer Chemistry Series, Royal Society of Chemistry, 2018, pp. 1–27.
[24] A. Poma, A. Guerreiro, M.J. Whitcombe, E.V. Piletska, A.P.F. Turner, S.A. Piletsky, Solid-phase synthesis of molecular imprinted polymer nanoparticles with a reusable template - "plastic antibodies", Adv. Funct. Mater. 23 (2013) 2817–2821.
[25] M.V. Sullivan, O. Clay, M.P. Moazami, J.K. Watts, N.W. Turner, Hybrid aptamer-molecularly imprinted polymer (aptaMIP) nanoparticles from protein recognition-A trypsin model, Macromol. Biosci. 21 (5) (2021), e2100002.
[26] D. Refaat, M.G. Aggour, A.A. Farghali, et al., Strategies for molecular imprinting and the evolution of MIP nanoparticles as plastic antibodies—synthesis and applications, Int. J. Mol. Sci. 20 (24) (2019) 6304.
[27] A. Poma, A. Guerreiro, M.J. Whitcombe, E.V. Piletska, A.P.F. Turner, S.A. Piletsky, Solid-phase synthesis of molecular imprinted polymer nanoarticles with a reusable template - "plastic antibodies.", Adv. Funct. Mater. 23 (22) (2013) 2817–2821.
[28] M.V. Sullivan, F. Allabush, H. Flynn, et al., Highly selective aptamer-molecularly imprinted polymer hybrids for recognition of SARS-CoV-2 spike protein variants, Glob Challenges. Published online March 20 (2023), 2200215, https://doi.org/10.1002/gch2.202200215.
[29] G. Erturk, B. Mattiasson, Molecular imprinting techniques used for the preparation of biosensors, Sensors 17 (2017) 288.
[30] V.L.V. Granado, M.T.S.R. Gomes, A. Rudnitskaya, Molecularly imprinted polymer thin-film electrochemical sensors, Methods Mol. Biol. 2027 (2019) 151–161.
[31] J.G. Drobny, Applications of Fluoropolymer Films: Properties, Processing, and Products, First. William Andrew Publishing, 2020.
[32] I.A. Nicholls, J. Rosengren, Molecular imprinting of surfaces, Bioseparation 10 (2001) 301–305.
[33] T.G. Traylor, S. Tsuchiya, Y.S. Byun, C. Kim, High-yield epoxidations with hydrogen peroxide and tert-butyl hydroperoxide catalysed by iron(III) porphyrins: heterolytic cleavage of hydroperoxides, J. Am. Chem. Soc. 115 (7) (1993) 2775–2781.
[34] W.S. Caughey, G.A. Smythe, D.H. Okeeffe, J.E. Maskasky, M.L. Smith, Heme-a of cytochrome-C oxidase - structure and properties - comparisons with Heme-B, Heme-C and Heme-S and derivatives, J. Biol. Chem. 250 (19) (1975) 7602–7622.
[35] P. Rothemund, A new porphyrin synthesis. The synthesis of porphin, J. Am. Chem. Soc. 58 (4) (1936) 625–627.
[36] J.T. Groves, Z. Gross, M. Stern, Prearation and reactivity of oxoiron(IV) porphyrins, Inorg. Chem. 33 (22) (1994) 5065–5072.
[37] C. Tanielian, C. Wolff, Porphyrin-sentized generation of singletet molecular oxygen: comparison of steady-state and time-resolved methods, J. Phys. Chem. 99 (24) (1995) 9825–9830.
[38] T.G. Traylor, F. Xu, A biomimetic model for catalases: the mechanisms of reaction of hydrogen peroxide and hydroperoxides with iron (III) porphyrins, J. Am. Chem. Soc. 109 (20) (1987) 6201–6202.
[39] J. Matsui, M. Higashi, T. Takeuchi, Molecular imprinted polymer as 9-ethyladenine receptor having a porphyrin-based recognition center, J. Am. Chem. Soc. 122 (21) (2000) 5218–5219.
[40] L. Longo, G. Vasapollo, Phthalocyanine-based molecular imprinted polymers as nucleoside receptors, Met Based Drugs 2008 (2008).
[41] T. Takeuchi, T. Mukawa, J. Matsui, M. Higashi, K. Shimizu, Molecular imprinted polymers with matalloporphryin-based molecular recognition sites coassembled with methacrylic acid, Anal. Chem. 73 (16) (2001) 3869–3874.

[42] H.F. EL-Sharif, H. Yapati, S. Kalluru, S.M. Reddy, Highly selective BSA imprinted polyacrylamide hydrogels facilitated by a metal-coding MIP approach, Acta Biomater. 28 (2015) 121–127, https://doi.org/10.1016/j.actbio.2015.09.012.
[43] D. Kotlarek, K. Liu, N.G. Quilis, et al., Thin-film polyisocyanide-based hydrogels for affinity biosensors, J. Phys. Chem. C 125 (23) (2021) 12960–12967, https://doi.org/10.1021/acs.jpcc.1c02489.
[44] C. Liu, T. Kubo, K. Otsuka, Specific recognition of a target protein, cytochrome c , using molecularly imprinted hydrogels, J. Mater. Chem. B 10 (35) (2022) 6800–6807, https://doi.org/10.1039/D2TB00501H.
[45] Y. He, X. Zhang, L. Cui, J. Wang, X. Fan, Catalyst-free synthesis of diversely substituted 6H-benzo[c]chromenes and 6H-benzo[c]chromen-6-ones in aqueous media under MWI, Green Chem. 14 (2012) 3429–3435.
[46] A.D. Alder, F.R. Longo, On the preparation of metalloporphyrins, J. Inorg. Nucl. Chem. 32 (7) (1970) 2443–2445.
[47] A.D. Alder, F.R. Longo, J.D. Finarelli, J. Goldmacher, J. Assour, L. Korsakoff, A simplified synthesis for meso-tetraphenylporphine, J. Org. Chem. 32 (2) (1967) 476.
[48] M. Zayats, A.J. Brenner, P.C. Searson, Protein imprinting in polyacrylamide-based gels, Biomaterials 35 (30) (2014) 8659–8668, https://doi.org/10.1016/j.biomaterials.2014.05.079.
[49] O. Kimhi, H. Bianco-Peled, Study of the interactions between protein-imprinted hydrogels and their templates, Langmuir 23 (11) (2007) 6329–6335.
[50] E. Verheyen, J.P. Schillemans, M. Van Wijk, M.A. Demeniex, W.E. Hennink, C. F. Van Nostrum, Challenges for the Effective Molecular Imprinting of Proteins 32 (11) (2011) 3008–3020.
[51] R.G. Brereton, ANOVA tables and statistical significance of models, J. Chemom. 33 (3) (2019), e3019, https://doi.org/10.1002/cem.3019.
[52] H. El-Sharif, H. Yapati, S. Kalluru, S.M. Reddy, Highly selective BSA imprinted polyacrylamide hydrogels facilitated by a metal-coding MIP approach, Acta Biomater. 28 (2015) 121–127.